Electronic Supplementary Material (ESI) for Nanoscale.

Electronic Supplementary Information

Iron-oxide-based twin nanoplates with strong T_2 relaxation shortening for contrast-enhanced magnetic resonance imaging

Ruixue Wei,[a] Tiantian Zhou,[b] Chengjie Sun,[a] Hongyu Lin,[a] Lijiao Yang,[a] Bin W. Ren,[a] Zhong Chen,[b] and Jinhao Gao*[a]

[a]State Key Laboratory of Physical Chemistry of Solid Surfaces, The MOE Laboratory of Spectrochemical Analysis & Instrumentation, and The Key Laboratory for Chemical Biology of Fujian Province, College of Chemistry and Chemical Engineering, Xiamen University, Xiamen 361005, China.

[b]Fujian Key Laboratory of Plasma and Magnetic Resonance, College of Electronic Science and Technology, Xiamen University, Xiamen 361005, China.

*Email: jhgao@xmu.edu.cn

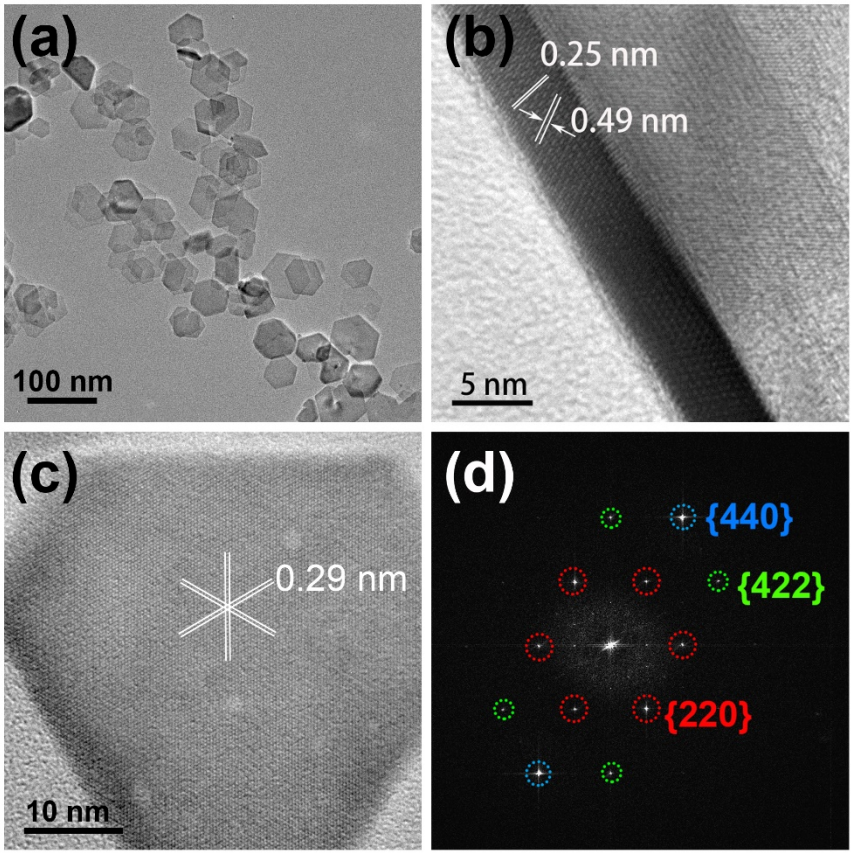

Fig. S1 A TEM image, HRTEM images and fast fourier transform (FFT) patterns of iron oxide nanoplates with thickness of 3 nm (IOP-3). (a) A TEM image of IOP-3. (b) A side-view HRTEM image of IOP-3, the lattice spacing distance of 0.25 nm and 0.49 nm could be ascribed to the {311} plane and {111} plane, respectively. The crystal zone could be ascribed to $[0\bar{1}1]$. (c) A top-view HRTEM image of IOP-3, the crossed lattice spacing distance of 0.29 nm could be attributed to the {220} plane. (d) FFT patterns of (c), showing {111} facets of face-centered cubic (FCC) crystals

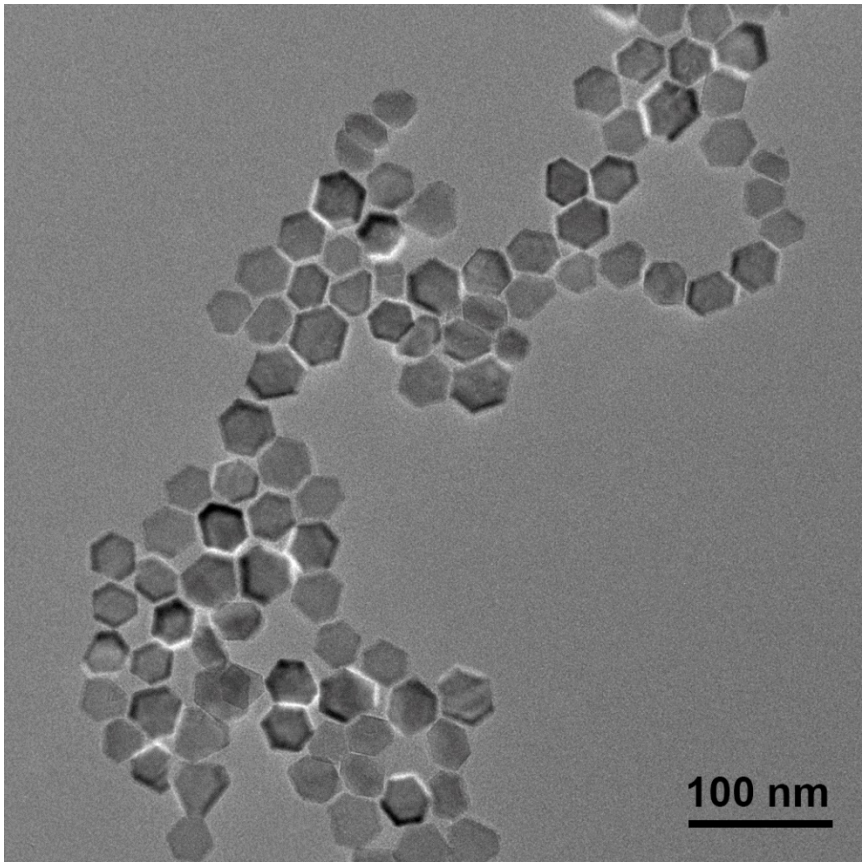

Fig. S2 A large-area TEM image of IOP-13.

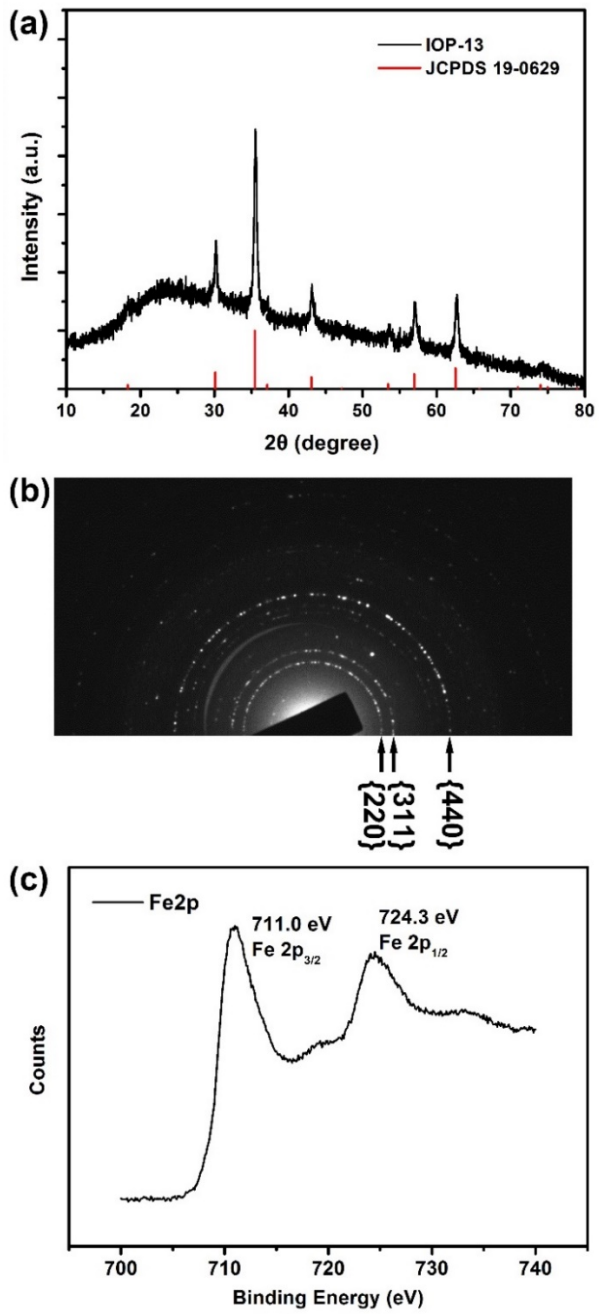

Fig. S3 (a) X-ray power diffraction (XRD) patterns of IOP-13, the diffraction patterns are in agreement with the magnetite structure (JCPDS NO. 19-0629). Selected area electron diffraction (SAED) patterns (b) and X-ray photoelectron spectroscopy (XPS) (c) of IOP-13 are also consistent with the crystalline nature of magnetite. The peaks of 711.0 and 724.3 eV are assigned to Fe 2p3/2 and Fe $2p_{1/2}$ of magnetite.

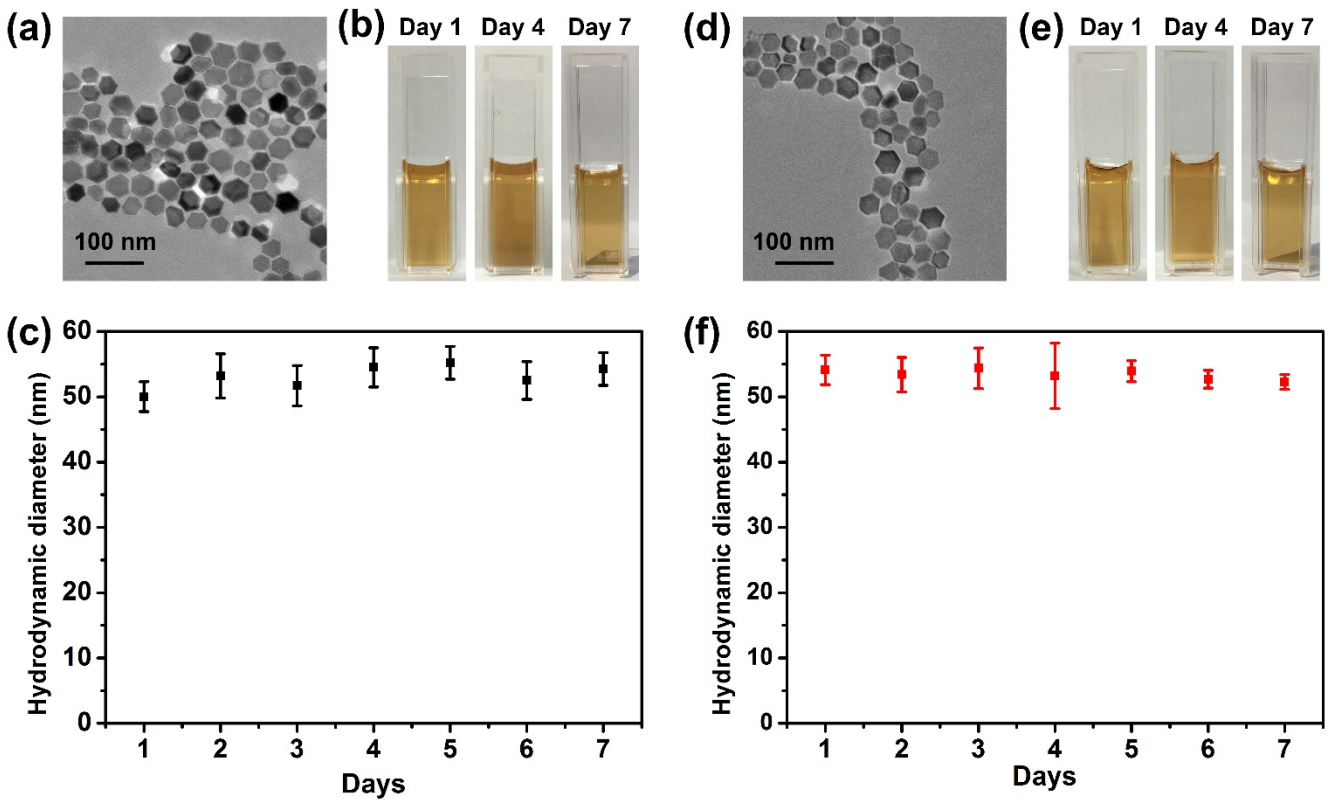

Fig. S4 The stability of IOP-13 in (a-c) phosphate buffer (PBS, 1×, pH = 7.4) and (d-f) 10% (v/v) fetal bovine serum (FBS) solution. The TEM images of IOP-13 after 7 days incubated with PBS (a) and FBS solution (d). The optical photographs of IOP-13 after incubated with PBS (b) and FBS solution (e). The hydrodynamic diameters of IOP-13 in PBS (c) and FBS solution (f) at different time points.

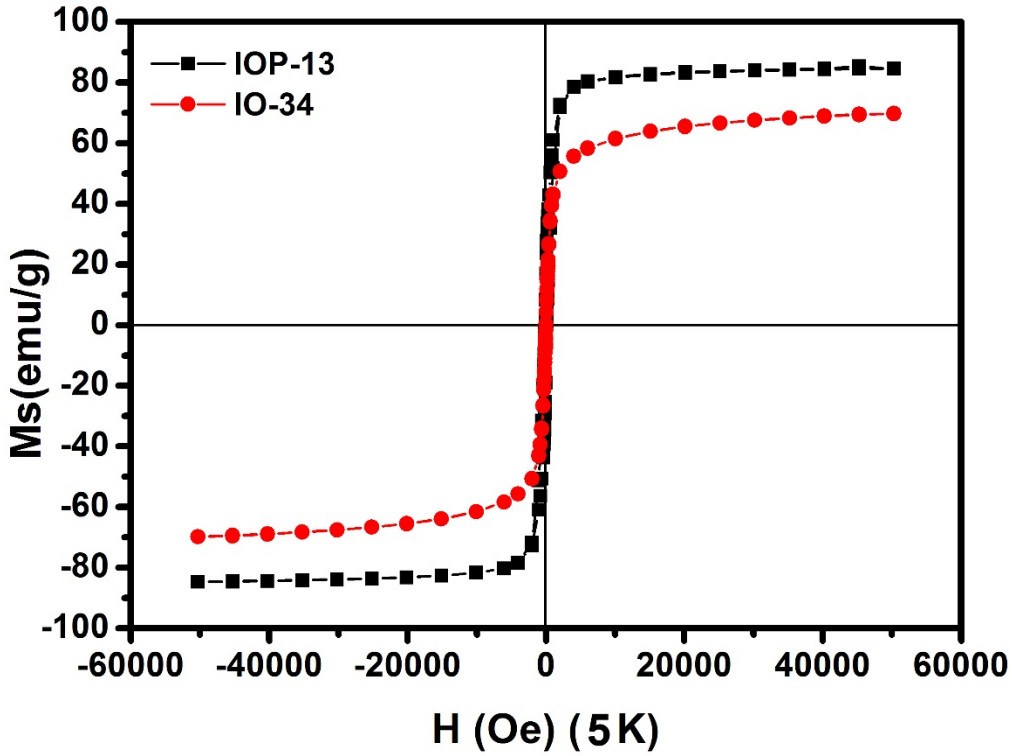

Fig. S5 Field-dependent magnetization curves (M−H) of IOP-13 at 5 K. The M_S of IOP-13 and IO-34 are 84.4 and 69.7 emu/g, respectively.

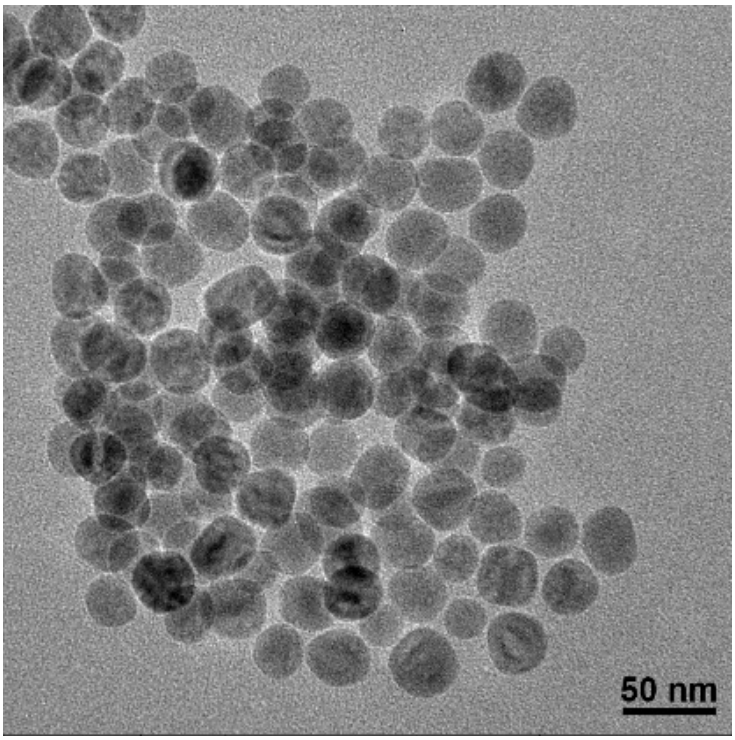

Fig. S6 A TEM image of as-prepared Fe_3O_4 nanoparticles (IO-34).

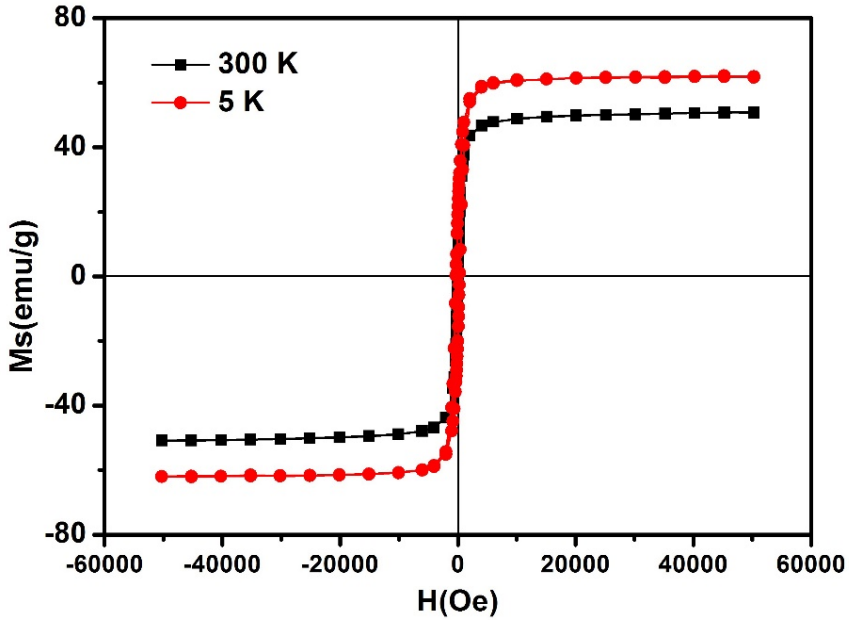

Fig. S7 Field-dependent magnetization curves (*M*−*H*) of IOP-3 seeds at 300 K and 5 K.

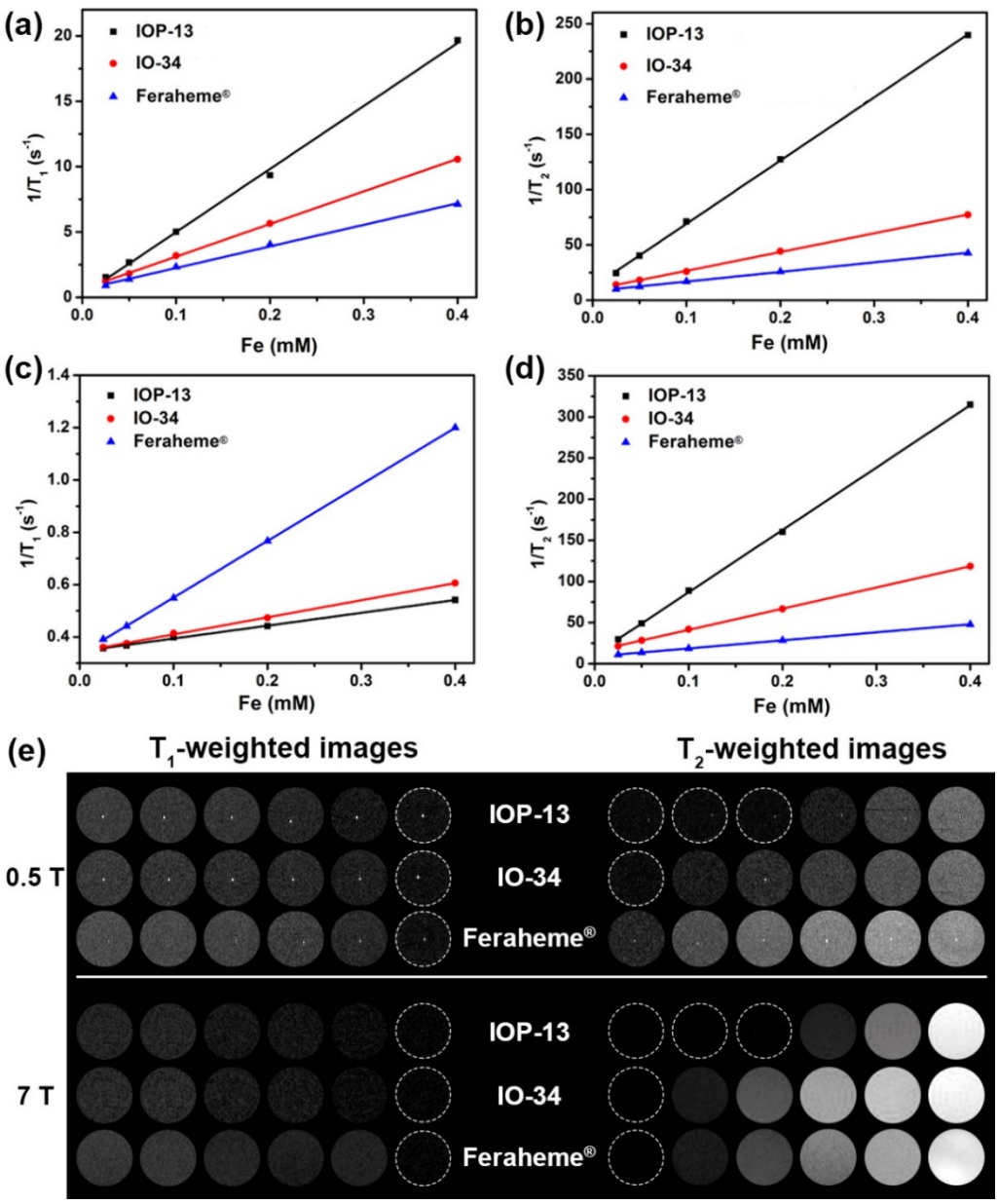

Fig. S8 Relaxivity profiles, T_1- and T_2-weighted phantom imaging at 0.5 and 7 T. (a) R_1 and (b) R_2 of IOP-13, IO-34, and Feraheme® with different concentrations at 0.5 T, the r_1 and r_2 values were obtained from the slopes of linear fits. (c) R_1 and (d) R_2 of IOP-13, IO-34, and Feraheme® with different concentrations at 7 T, the r_1 and r_2 values were obtained from the slopes of linear fits. (e) T_1-/T_2-weighted phantom imaging of IOP-13, IO-34, and Feraheme® at 0.5 and 7 T.

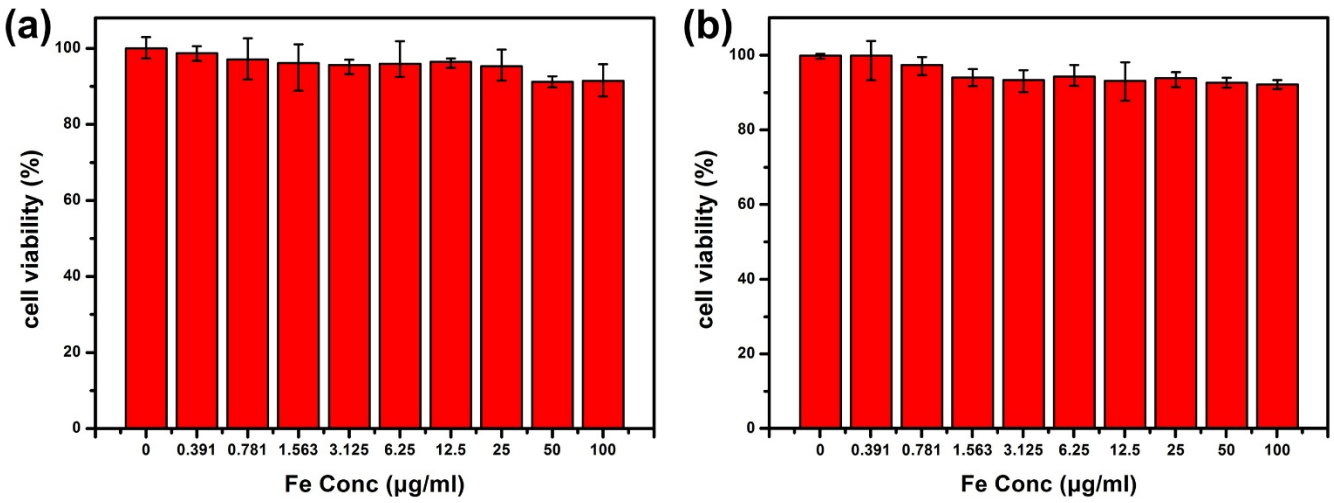

Fig. S9 Cell viability of SMMC-7721 cells incubated with various concentrations of (a) Fe_3O_4 nanoplates (IOP-13) and (b) Fe_3O_4 nanoparticles (IO-34) for 24 h. The results show that the cell viabilities are more than 90% even at the concentration of 100 μg [Fe] mL^{-1}, indicating that IOP-13 and IO-34 have no appreciable cytotoxicity and excellent biocompatibility.

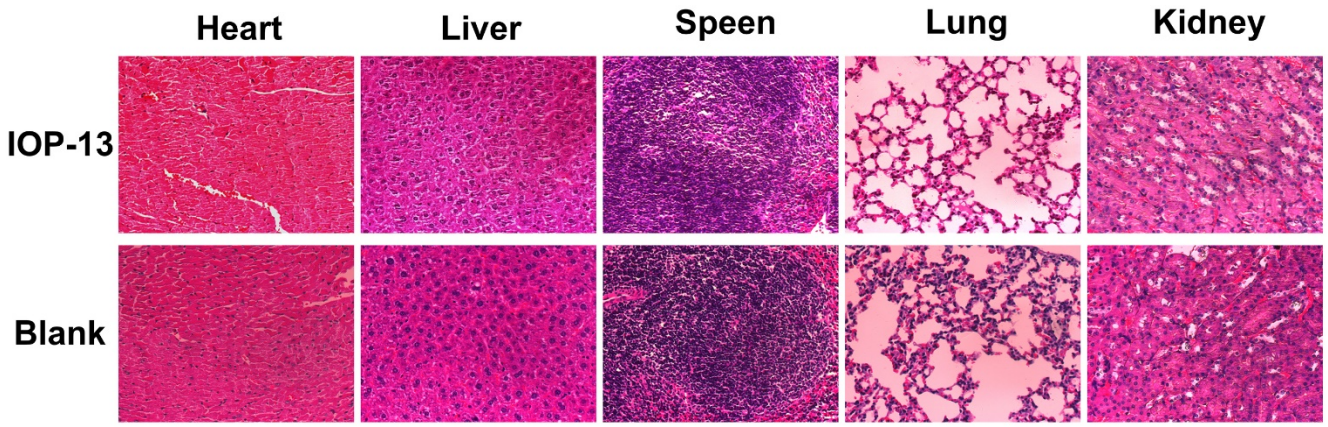

Fig. S10 Hematoxylin and eosin (H&E) staining of heart, liver, spleen, lung, and kidney of the mice after administration of IOP-13 at a dose of 20 mg Fe per kg body weight. The mice of the control group were injected with the same volume of 1 × PBS.

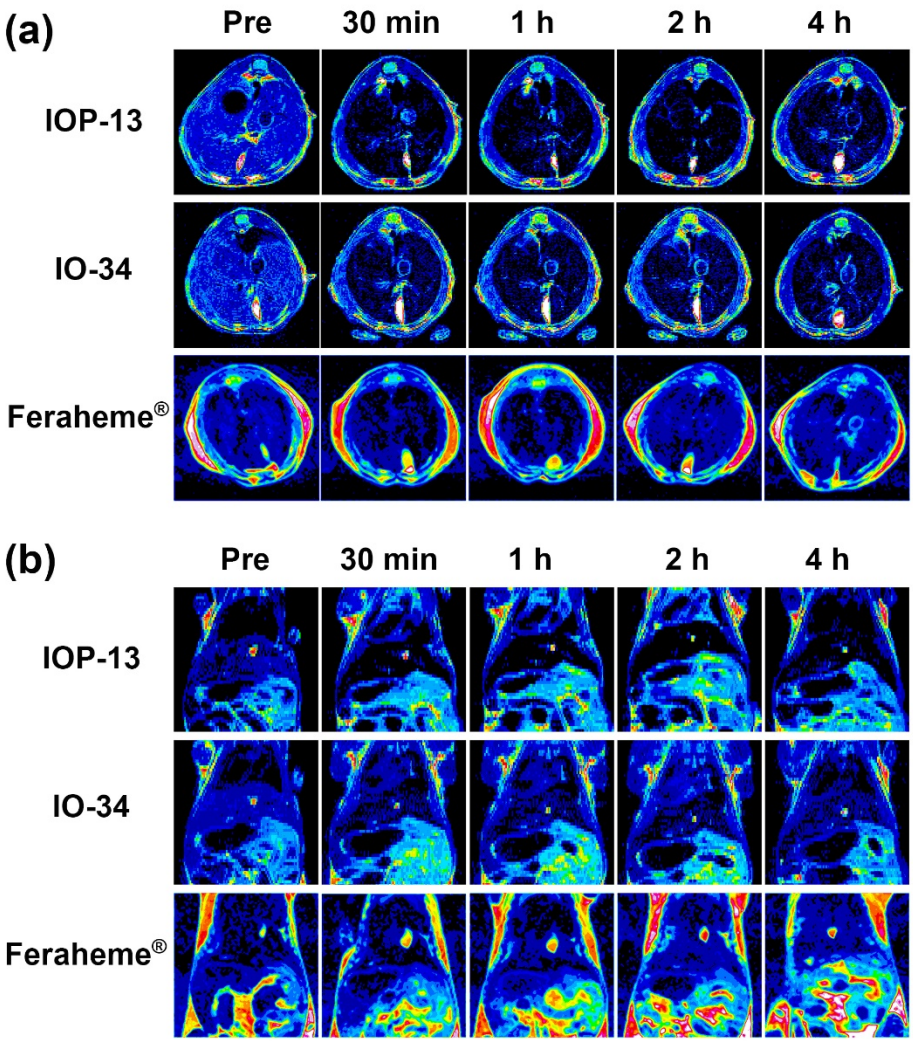

Fig. S11 *In vivo* T_2-weighted MR false-color images of liver at 7.0 T. (a) T_2-weighted MR false-color images in the transverse plane at 0, 0.5, 1, 2, and 4 h after intravenous injection of IOP-13, IO-34 nanoparticles and Feraheme® at a dose of 2 mg [Fe]/kg body weight. (b) T_2-weighted MR false-color images in the coronal plane at 0, 0.5, 1, 2, and 4 h after intravenous injection of IOP-13 and IO-34 nanoparticles at a dose of 2 mg [Fe]/kg body weight.

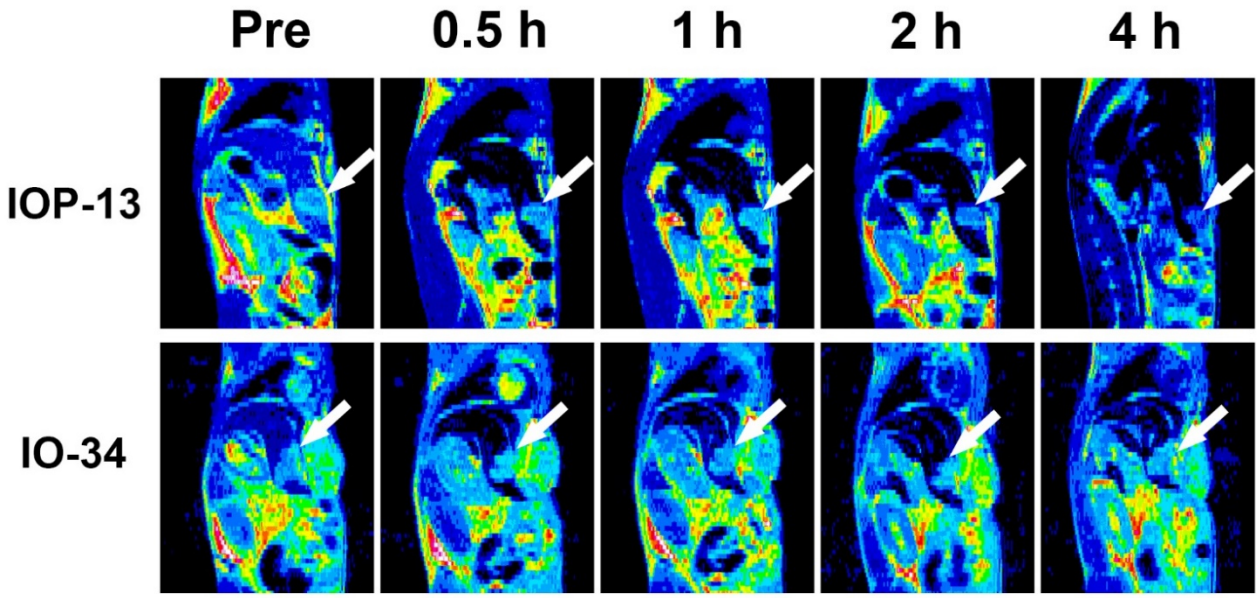

Fig. S12 *In vivo* T_2-weighted MR false-color images of liver tumor at 7.0 T. T_2-weighted MR false-color images in the sagittal plane at 0, 0.5, 1, 2, and 4 h after intravenous injection of IOP-13 and IO-34 nanoparticles at a dose of 2 mg [Fe]/kg body weight. Arrows indicate the location of tumor.

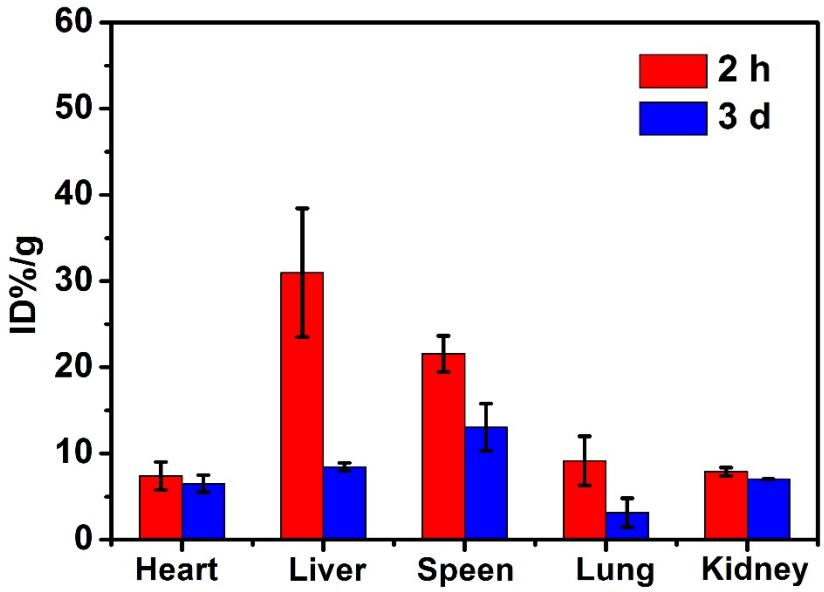

Fig. S13 Biodistribution of IOP-13 in mice organs at 2 h and 3 d after intravenous injection (2 mg Fe /kg body weight, *n* = 3/group). The iron contents were measured by ICP-MS and the background was subtracted.

Table S1. The r_1 and r_2 values of IOP-13, IO-34, and Feraheme® at 0.5 and 7.0 T.

Sample	r_1 ($mM^{-1}s^{-1}$)		r_2 ($mM^{-1}s^{-1}$)		r_2/r_1	
	0.5 T	7 T	0.5 T	7 T	0.5 T	7 T
IOP-13	48.21	0.49	571.21	758.04	11.85	1547.02
IO-34	24.93	0.65	161.02	257.52	6.48	396.18
Feraheme®	16.49	2.16	86.85	98.45	5.27	45.57